



Cu(II)-Based Ionic Liquid Supported on SBA-15 Nanoparticles Catalyst for the Oxidation of Various Alcohols into Carboxylic Acids in the Presence of CO₂

Qi Peng¹ · Dejian Hou² · Yanwu Chen¹ · Litian Lin³ · Seyed Mohsen Sadeghzadeh⁴

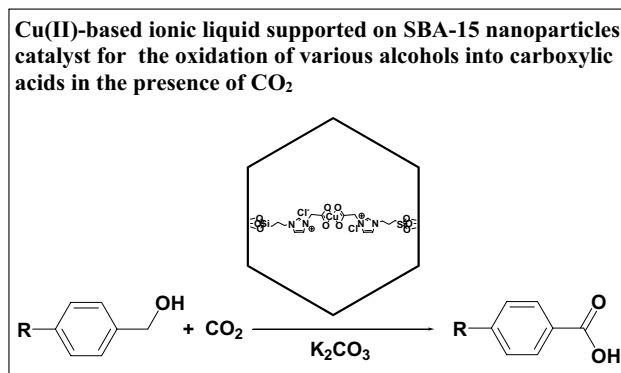
Received: 17 March 2021 / Accepted: 8 July 2021

© The Author(s), under exclusive licence to Springer Science+Business Media, LLC, part of Springer Nature 2021

Abstract

In this paper, we have produced carboxylic acids by the oxidation of various alcohols in the presence of CO₂ using SBA-15/IL supported Cu(II) (SBA-15/IL/Cu(II)) as nanocatalyst. The obtained products showed to have excellent yields by taking into account of SBA-15/IL/Cu(II) nanocatalyst. In addition, the analysis of EDX, SEM, TGA, TEM, XPS, and FT-IR showed the heterogeneous structure of SBA-15/IL/Cu(II) catalyst. It is determined that, after using SBA-15 excess, the catalytic stability of the system was enhanced. Moreover, hot filtration provided a full vision in the heterogeneous catalyst nature. The recycling as well as reuse of the catalyst were studied in cases of coupling reactions many times. Moreover, we have studied the mechanism of the coupling reactions.

Graphic Abstract



Keywords Nanocatalyst · Green chemistry · Carboxylic acids · SBA-15 · Carbon dioxide

✉ Qi Peng
cheese_pp@126.com

✉ Seyed Mohsen Sadeghzadeh
seyedmohsen.sadeghzadeh@gmail.com

¹ College of Light Chemical Engineering and Materials, Shunde Polytechnic, Foshan 528300, China

² School of Materials Science and Engineering, Hanshan Normal University, Chaozhou 521041, China

³ Guangdong Province Key Laboratory of Rare Earth Development and Application, Institute of Rare Metals, Guangdong Academy of Sciences, Guangzhou 510651, China

⁴ Department of Chemistry, Faculty of Sciences, Neyshabur Branch, Islamic Azad University, Neyshabur, Iran

1 Introduction

Different Cu(I) based heterogeneous catalysts has been introduced like copper nanocluster [1], copper(I), a copper manganese spinel oxide [2], zeolites [3], Cu₂O and Cu/C [4] on water [5]. In addition, the facet dependent catalytic potential of Cu₂O nanocrystals are proved to the regioselective synthesis of focused 1,4-disubstituted 1,2,3-triazoles in green media [6]. In the literature, Lautens and his group introduced the intramolecular Cu(I)-catalyzed terminated click–acylation domino reaction [7]. In the reference [8], researchers have investigated the use of copper NPs as catalyst to produce 1,4-disubstituted 1,2,3-triazoles in water. In the reference [9], researchers have investigated the use of catalyst Cu(OAc)₂ for 1,3-dipolar cycloaddition reactions by special focus on chelating ligands. In the recent years, in order to obtain the appropriate 1,2,3-triazole evoked the particular interest for Cu(II) catalysts, researchers suggested Cu(II) acetate precatalysts and Cu(II)-trenprecatalysts for the 1,3-dipolar cycloaddition reactions [10, 11]. Despite several advances, scholars have not yet proposed a reaction method that does not require the use of explosive azides and is suitable for recyclable catalysts, single step reactions, atom economy.

Mesoporous silica materials can be used as a platform for many applications in diagnosis, therapeutics and pharmaceuticals [12]. SBA-15 as a mesoporous silica material, is widely utilized as supports in the case of heterogeneous catalysis due to the dispersity of active sites. In addition, for increasing the efficiency of mentioned materials, one can cofunctionalize them by other functional groups [13–15]. Moreover, SBA-15 can be utilized in wastewater purification, treatment and gas separation [16]. It is mesopore-rich and showed to have considerable internal surface area, high hydrothermal, plentiful surface hydroxyl groups and appropriate mechanical stability. Currently, in cases of catalyze reactions, a substantial number of catalysts like ionic liquids (ILs) [17, 18] as well as transition metal complexes [19, 20] were evaluated to be immobilized on SBA-15. Moreover, these immobilized catalysts demonstrated appropriate recyclability. SBA-15 is thought to be proper choice for stably-supporting multi-site ILs due to having mesoporous channel and plain loading [21–24].

In the process of catalysis synthesis, dendrimers are widely utilized due to having unique dendritic effects, abundant peripheral groups and high branched tridimensional structures [25, 26]. The use of dendrimer catalyst onto support materials was introduced as a new field of study and many researchers investigated it due to their easy reusability and recoverability [27–29]. Ionic liquids (ILs) are highly suggested in green chemistry because of their unparalleled attributes such as good stability, low

flammability, low vapour pressure. ILs have adjustable structure and properties known as the most significant characteristic of them. Many functional groups in cations/anions with different structures can be used to adjust the physical and chemical characteristics of them. In dendritic ILs (DILs), the properties of dendrimers and ILs are combine. DILs are widely utilized in the processes of adsorption of heavy metal cations, catalysis and transporters [30, 31].

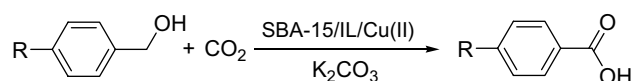
Synthesis of carboxylic acids from oxidation of alcohols is a significant methods for the preparation of different fine chemicals in the chemical industry, and has been kept a difficult task in the field of green organic synthesis [32]. Stoichiometric, traditionally, expensive oxidants, and toxic, such as CrO₃ [33], and KMnO₄ [34] have often been used to complete this conversion, resulting in significant waste. Therefore, it is highly desirable to develop an environmentally friendly new oxidation scheme. Compared with traditional oxidants, the non-toxic nature, cheap, and abundant of carbon dioxide has brought great interest to its use as an accelerator in oxidation reactions, including the oxidative dehydrogenation of alkanes, the oxidation of alkyl aromatics, CH₄, C–C bond formation between aldehydes and the like [35]. Although metal–ligand complexes have become a mature technology for the selective catalytic oxidation of alcohols to aldehydes [36–38], there are few reports on the oxidation of alcohols directly to carboxylic acids.

Here, a novel and green approach is suggested to produce SBA-15 nanoparticles (NPs), which is immobilized using ionic liquid supported Cu(II) since IL/Cu(II) has a structure like cage that utilized as an eco-friendly, inexpensive, non-toxic ligand and highly reactive or catalyst to different ionic liquids. The mentioned catalyst possessed many priorities such as good activity, selectivity and easy separation for activating CO₂ with taking into account of mild conditions. In the present work, the first example of the application of SBA-15/IL/Cu(II) catalyst is suggested for oxidation of various alcohols into carboxylic acids (refer to Scheme 1).

2 Experimental

2.1 Materials and Methods

Chemical materials were purchased from Fluka and Merck in high purity. Melting points were determined in open capillaries using an Electrothermal 9100 apparatus and are uncorrected.



Scheme 1 Oxidation of various alcohols into carboxylic acids in the presence of SBA-15/IL/Cu(II)

FTIR spectra were recorded on a VERTEX 70 spectrometer (Bruker) in the transmission mode in spectroscopic grade KBr pellets for all the powders. The particle size and structure of nano particle was observed by using a Philips CM10 transmission electron microscope operating at 100 kV. Powder X-ray diffraction data were obtained using Bruker D8 Advance model with Cu ka radiation. The thermogravimetric analysis (TGA) was carried out on a NETZSCH STA449F3 at a heating rate of 10 °C min⁻¹ under nitrogen. ¹H and ¹³C NMR spectra were recorded on a BRUKER DRX-300 AVANCE spectrometer at 300.13 and 75.46 MHz, BRUKER DRX-400 AVANCE spectrometer at 400.22 and 100.63 MHz, respectively. Elemental analyses for C, H, and N were performed using a Heraeus CHN-O-Rapid analyzer. The purity determination of the products and reaction monitoring were accomplished by TLC on silica gel polygram SILG/UV 254 plates. Mass spectra were recorded on Shimadzu GCMS-QP5050 Mass Spectrometer.

2.2 General Approach for the Synthesis of SBA-15 NPs

SBA-15 is produced based on the reference [39]. Tetraethyl orthosilicate (TEOS) is utilized as silica source and Pluronic (P123) is utilized as template. Firstly, 8.0 g of P123 and a constant amount of TEOS equal to 17.0 g are slowly added to an aqueous solution of HCl (2 mol/L, 240 mL) along with 60 g of water. For a day, whole considered mixtures is stirred under the temperature of 40 °C and after that was heated to the temperature of 100 °C for another 24 h considering static conditions. In the next step, the mesoporous material is filtered, washed by water up to when no Cl⁻ is not detected. The result compound is dried under the temperature of 40 °C considering vacuum condition. After that, the dried sample is dissolved in methanol and sonicated under the temperature of 40 °C for 20 min, then was filtered and repeated for three times. In the last step, the resulted compound is dried under vacuum under the temperature of 40 °C for obtaining SBA-15.

2.3 The Universal Approach to Provide SBA-15/3-Bromopropyl NPs

The SBA-15 (3.0 g) was released into the solution of NaOH (50 mL, 0.5 M), and the blend was refluxed for 3 h to enhance hydrophilicity. Then, the resulting nanoparticles were cleansed several times with H₂O to neutralize the pH of the deionized H₂O and then vacuum-dried at 70 °C for 6 h. Next, 3-bromopropyltrimethoxysilane was supported on the SBA-15 exterior layer to synthesis amino-modified SBA-15/3-bromopropyl. A blend of activated SBA-15 (4 g) and 3-bromopropyltrimethoxysilane (7 mL) in 100 mL ethanol was mixed at 100 °C for 17 h. In the last step,

SBA-15/3-Bromopropyl was filtered, cleansed twice with deionized water, and dried at 90 °C for 12 h.

2.4 The Universal Approach to Provide SBA-15/IL NPs

The 4 g of SBA-15/3-Bromopropyl was suspended in 1-imidazole (3.0 g), tetrahydrofuran (50.0 mL) was released, and the blend was mixed at 70 °C for 20 h. SBA-15/Imidazole (80 mg) was released into deionized water. EtOH blend (5:5 v/v, 80 mL) contained 2-chloroacetic acid (3.0 g), and the reaction was performed at r.t. for 2.5 h. Upon separating the solvent, the final blend was filtered. Then the filtrate was vacuum-dried at 50 °C.

2.5 The Universal Approach to Provide SBA-15/IL/Cu (II)

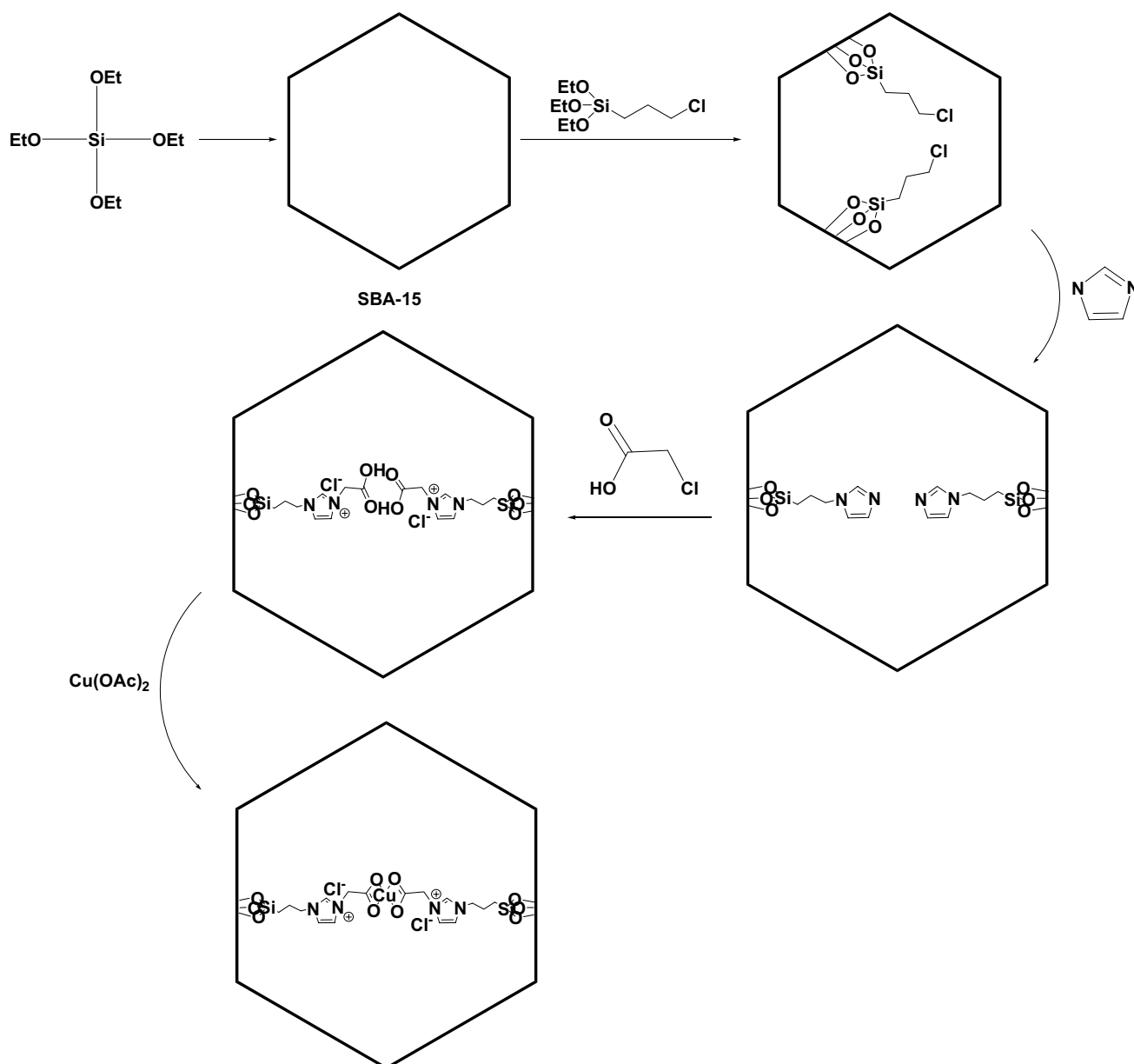
Cu(OAc)₂ (0.15 g) was released to a blend of SBA-15/IL (0.25 g) in 25 mL of ethanol and then mixed for 3 h at r.t. Next, the ethanol was removed under decreased pressure and the remnant was cleansed first with Et₂O, then with CH₂Cl₂:Et₂O (4:1 v/v), and finally with Diethylether:Acetone (1:1 v/v) to give an orange solid.

2.6 General Procedure for Oxidation of Alcohols

Aryl alcohols (1 mmol), SBA-15/IL/Cu (II) NPs (7 mg), and K₂CO₃ (5 mmol) in 5 mL of DMSO were mixed in a 200 mL autoclave. Purified twice with CO₂ gas, pressurized with 1.5 MPa of CO₂, and then heated under 60 °C for 12 h. Upon completion of the reaction, the reaction mixture was cooled to r.t. Remaining CO₂ was carefully evacuated. The progress of the reaction was monitored by TLC. EtOH was released into the reaction blend and the SBA-15/IL/Cu (II) was isolated. The solvent was then separated under decreased pressure and the final carboxylic acids was purified by recrystallization employing ethyl acetate/*n*-hexane.

3 Results and Discussion

The production of the SBA-15/IL/Cu (II) nanocatalysts included many different stages (refer to Scheme 2). The SBA-15/3-chloropropylsilane NPs (SBA-15) fibers showed to have different Si-OH groups onto the surface. Hence, we expected that the SBA-15 fibers can be simply functionalized by 3-chloropropyltriethoxysilane for the formation of SBA-15/3-chloropropylsilane NPs. After that, we loaded imidazole as well as 2-chloro acetic acid in SBA-15/IL NPs. The recyclable catalyst of SBA-15/IL supported copper (II) is produced in aqueous solutions



Scheme 2 Preparation of SBA-15/IL/Cu(II) nanocatalyst

that demonstrates by easy availability of active sites along with high catalytic activity is produced using a simple, cost-effective approach.

Moreover, SEM and TEM analysis are used to characterize the morphology and also pore structure of the SBA-15 and SBA-15/IL/Cu(II). Figure 1a and c shows the SEM and TEM images of SBA-15. In addition, Fig. 1b and d shows the SEM and TEM images of immobilized IL/Cu(II) catalysts. As seen, the strip sharp and regular appearance of SBA-15 and hexagonal structure of SBA-15 is clear, demonstrating the usual structure of SBA-15 [12]. Moreover, after loading IL/Cu(II), the SBA-15 structure have not varied.

As shown in Fig. 2, the mesoporous structure can be clearly observed in the HAADF-STEM image. In the elemental maps for the hybrid material, the colors for O, N, Si, and Cu were uniformly dispersed and the adsorbed Cu(II) was found in similar areas to the other elements. This confirmed that Cu(II) was adsorbed from the solution by the grafted ligands and homogeneously distributed within the inner channels of the SBA-15.

As can be seen in Fig. 3, the decomposition conduct of the SBA-15 as well as IL/Cu(II) catalysts SBA-15/IL/Cu(II) is compared for understanding the influences of the grafted dendritic IL molecules. In Fig. 3, the TGA analysis

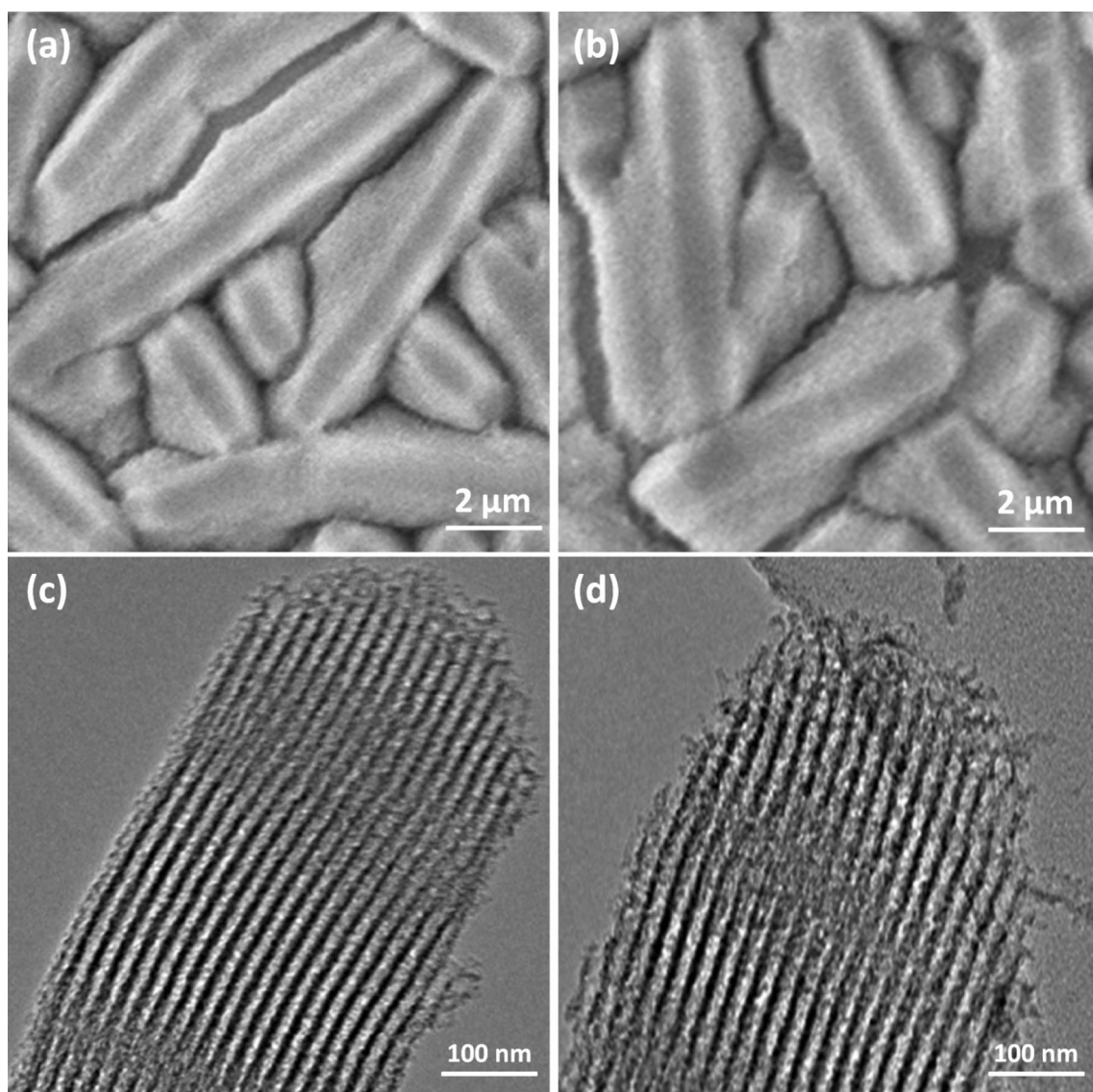


Fig. 1 SEM images of **a** SBA-15; and **b** SBA-15/IL/Cu(II) NPs; TEM images of **c** SBA-15; and **d** SBA-15/IL/Cu(II) NPs

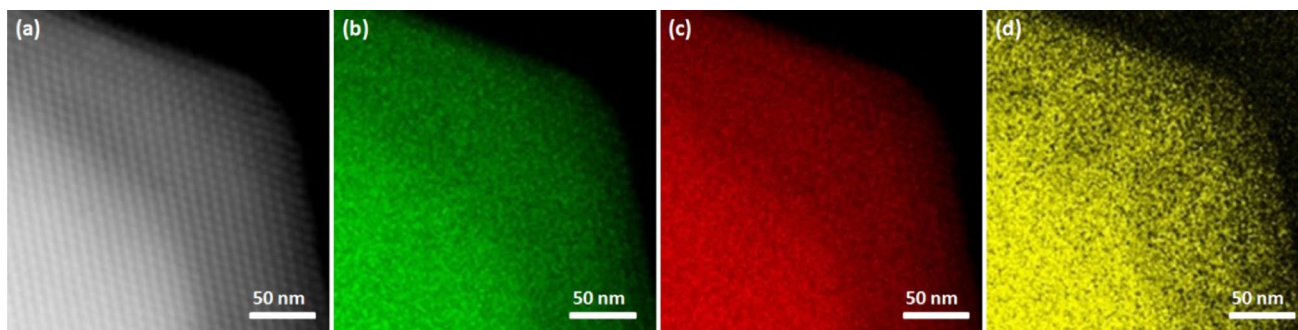
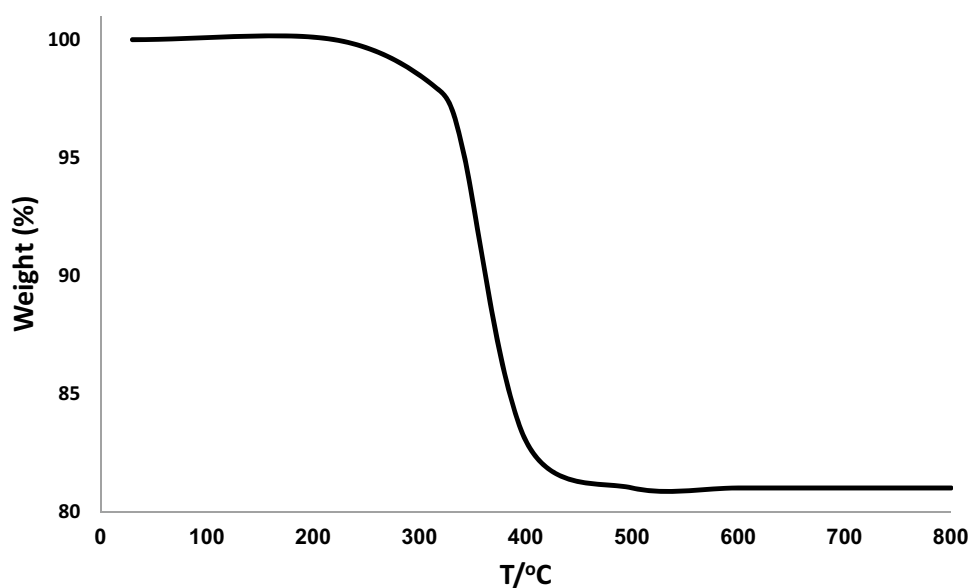


Fig. 2 HAADF-STEM image and the corresponding multi-element (Si, O and Cu) EDS mapping images of SBA-AP with Cu(II) adsorption

Fig. 3 TGA diagram of SBA-15/IL/Cu(II) NPs

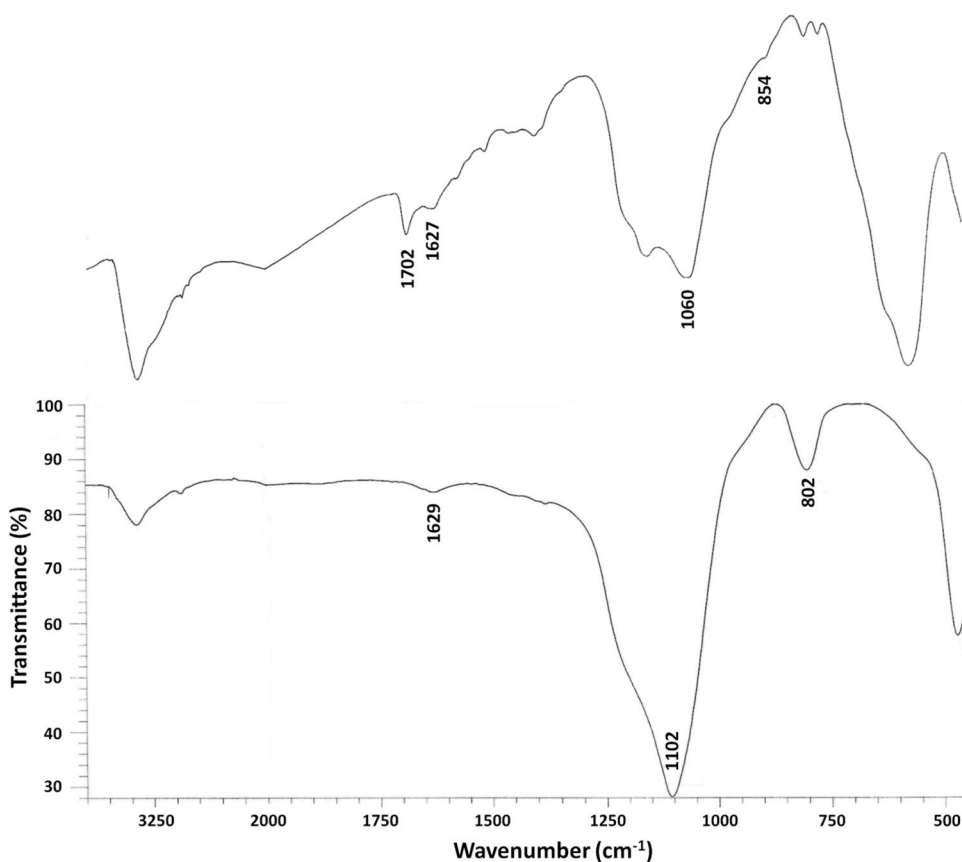


in the cases of SBA-15/IL/Cu(II) are shown. As seen in the TGA curves, there are two processes of weight loss that the first process is determined among 30 and 100 °C demonstrated small weight loss equal to 5.0% related to the evaporation of physical adsorbed H₂O from the samples. Second one is between 300 and 450 °C demonstrated

clear reduces by large weight loss of 22% related to the lignin degradation.

The spectroscopy of FT-IR is utilized for detecting possible variations in the exterior layer of the produced catalyst (refer to Fig. 4). As can be seen in Fig. 4a, in the spectrum of FT-IR in the case of SBA-15, the bands of 1629, 1102,

Fig. 4 FTIR spectra of SBA-15 (a); SBA-15/IL/Cu(II) NPs (b)



and 802 cm^{-1} stands for the tensile state of the water, which is absorbed onto the exterior layer of solid, Si–O–Si vibrations, and Si–OH, respectively. As can be seen in Fig. 4b, there are many new absorption peaks demonstrated at 1702 , 1060 , and 854 cm^{-1} in comparison to the FT-IR spectrum of luffa sponge revealed to the tensile vibration of Si–O bond as well as the flexural vibrations of C=N bond onto the SBA-15/IL exterior layer. In addition, the wide peak revealed at 1701 cm^{-1} is due to C=O tensile vibrations in the acetic acid functional states. Bands at 1627 cm^{-1} are due to the bending vibrations of N–H in the ammonium types. We have found that IL is properly immobilized on the nanoparticle of SBA-15.

In the present paper, XPS analysis was utilized for investigating the chemical sections on the SBA-15/IL/Cu(II) NPs level. In the case of considered catalyst, Fig. 5 shows XPS scheme. There are the peaks of Si, C, O, Cl, N, and Cu and

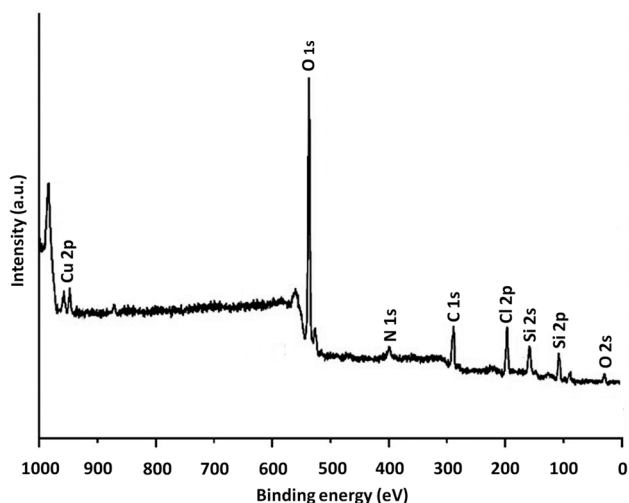


Fig. 5 XPS spectra of SBA-15/IL/Cu(II) NPs

the attendance of N 1 s additional proved that SBA-15 were functionalized by utilizing the imidazole. In addition, the existence of ions of Cl^- known as the 2-chloroacetic acid counter ion is characterized using a sharp peak proved copper moiety in the catalyst. In Fig. 6, in the catalyst, the origins are demonstrated that determined using the analysis of EDX. Figure 6 shows the EDX pattern of whole considered elements existed in SBA-15/IL/Cu(II) NPs such as silicon, carbon, oxygen, nitrogen, copper and chlorine.

Table 1 illustrates that the produced SBA-15 possessed similar properties as commercial the SBA-15 and SBA-15, before and after grafting demonstrates a considerable large difference. The typical IV-type containing the H1 hysteresis loop is exhibited by using the BET data (Fig. 7). In cases of SBA-15/IL/Cu(II), the surface areas of BET are determined to be $337\text{ m}^2\text{ g}^{-1}$; pore diameters are equal to 6.14 nm ; and pore volumes $0.54\text{ cm}^3\text{ g}^{-1}$, respectively. Compared to pristine SBA-15, the SBA-15/IL/Cu(II) nitrogen sorption analysis has demonstrated a regular and uniform mesostructure having a reduction of surface area, pore diameter and pore volume parameters. The related pore volumes were considerably decreased by the functionalization using Si-IL/Cu(II). As seen, IL/Cu(II) are immobilized onto SBA-15 that is related to reducing surface area as well as total pore volume, (refer to Table 1).

The catalytic activity of the different kinds of SBA-15/IL/Cu(II) are examined by oxidation of salicyl alcohol into carboxylic acid in the presence of CO_2 (refer to Table 2).

Table 1 Structural parameters of SBA-15, and SBA-15/IL/Cu(II) materials determined from nitrogen sorption experiments

Catalysts	$S_{\text{BET}}\text{ (m}^2\text{ g}^{-1}\text{)}$	$V_t\text{ (cm}^3\text{ g}^{-1}\text{)}$	$D_{\text{BJH}}\text{ (nm)}$
SBA-15	536	0.97	6.67
SBA-15/IL/Cu(II)	337	0.54	6.14

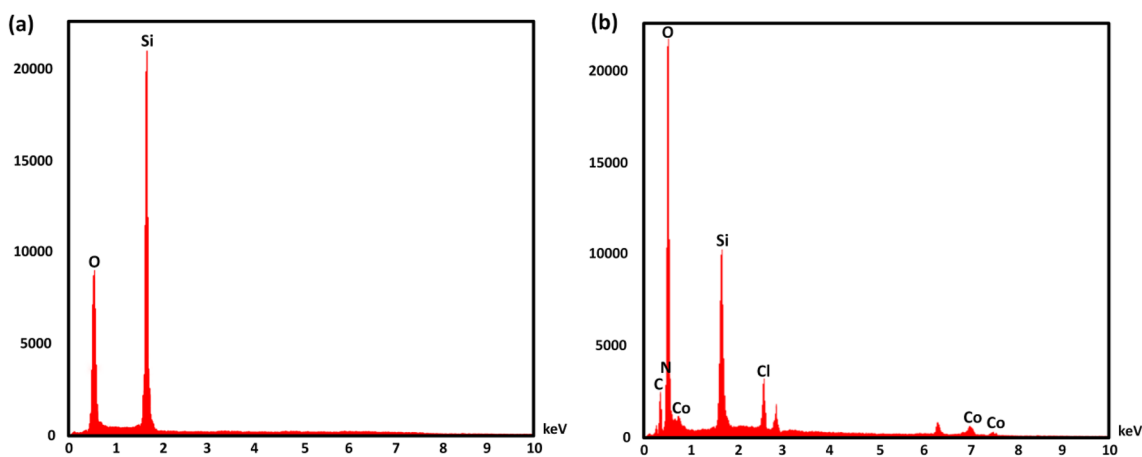


Fig. 6 EDX spectra of SBA-15 (a); SBA-15/IL/Cu(II) NPs (b)

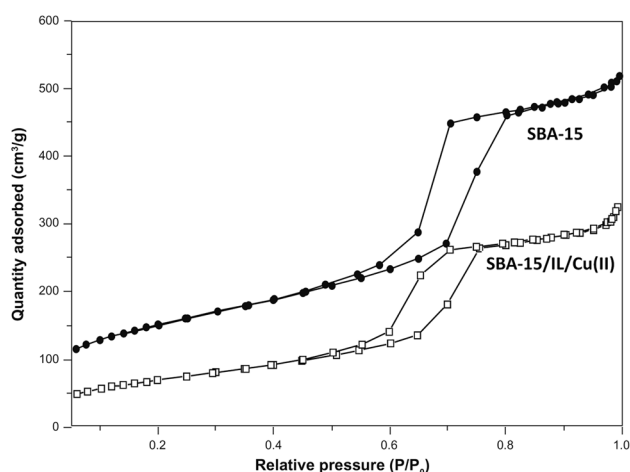


Fig. 7 The N_2 adsorption–desorption isotherms of SBA-15 and SBA-15/IL/Cu(II)

The effect of different elements like a time, and solvent on the model reaction and the impact of solvents on the oxidation were examined (Table 2, rows 1–14). According to the assessed outcomes of solvents, no quantity of the interested product was formed in the presence of polar protic solvents, like isopropanol, methanol, and ethanol. Nevertheless, the efficiency of the product was relatively moderate in the attendance of polar aprotic solvents, such as EtOAc, toluene, DMF, $CHCl_3$, and CH_2Cl_2 . Under standard conditions, DMSO acts more effectively compared to other solvents (Table 2, row 8). The results showed that K_2CO_3 is the most efficient base for oxidation of salicyl alcohol. Under optimal conditions, the reaction progress was monitored by GC to detect the minimum time required in the attendance of 10 mg of SBA-15/IL/Cu(II) NP. Results showed that the excellent production efficiency of carboxylic acid could be achieved in 12 h (Table 2, row 25). The screening of the quantity of K_2CO_3 depicted that 5.0 mmol was the premier option (Table 2, entries 28 and 29). Enhancing the quantity of base did not improved the results (Table 2, rows 25).

Catalyst loading is key determining element in the current reaction (Fig. 8). the oxidation reaction had low efficiency in the absence of a catalyst. When 3–5 mg of SBA-15/IL/Cu(II) NPs were added to the reaction, a moderate yield of oxidation reaction was achieved. The best result was obtained in the attendance of 7 mg of SBA-15/IL/Cu(II) NPs. Increasing the amount of catalyst did not show any improvement in the model reaction. No product was achieved in the nonattendance of the catalyst. The effects of CO_2 pressure in the attendance of salicyl alcohol and SBA-15/IL/Cu(II) NPs for 12 h are depicted in Fig. 9. The catalyst blend showed the highest efficiency (92%) at a pressure of 1.5 Mpa. No specific by-product was observed by GC in all the experiments and the salicyl alcohol oxidation reaction was acquired with

Table 2 Oxidation of salicyl alcohol by SBA-15/IL/Cu(II) NPs in different time, solvents, and bases

Entry	Solvent	Base	Base (mmol)	Time (h)	Yield (%) ^a
1	Solvent-free	K_2CO_3	7	16	–
2	EtOH	K_2CO_3	7	16	–
3	MeOH	K_2CO_3	7	16	–
4	<i>i</i> -PrOH	K_2CO_3	7	16	–
5	Dioxane	K_2CO_3	7	16	–
6	H_2O	K_2CO_3	7	16	–
7	<i>n</i> -Hexane	K_2CO_3	7	16	–
8	DMSO	K_2CO_3	7	16	92
9	EtOAc	K_2CO_3	7	16	17
10	DMF	K_2CO_3	7	16	62
11	THF	K_2CO_3	7	16	23
12	CH_3CN	K_2CO_3	7	16	46
13	CH_2Cl_2	K_2CO_3	7	16	32
14	$CHCl_3$	K_2CO_3	7	16	31
15	DMSO	–	7	16	–
16	DMSO	CsF	7	16	–
17	DMSO	Na_2CO_3	7	16	59
18	DMSO	Et_3N	7	16	–
19	DMSO	NaOAc	7	16	–
20	DMSO	KOH	7	16	34
21	DMSO	K_3PO_4	7	16	60
22	DMSO	Cs_2CO_3	7	16	77
23	DMSO	<i>t</i> BuOK	7	16	–
24	DMSO	K_2CO_3	7	14	92
25	DMSO	K_2CO_3	7	12	92
26	DMSO	K_2CO_3	7	10	86
27	DMSO	K_2CO_3	7	8	64
28	DMSO	K_2CO_3	5	12	92
29	DMSO	K_2CO_3	3	12	71

Reaction conditions: salicyl alcohol (1 mmol), K_2CO_3 (5 mmol), SBA-15/IL/Cu(II) NPs (10 mg), CO_2 (2 MPa), solvent (15 mL), under 80 °C

^aIsolated yields

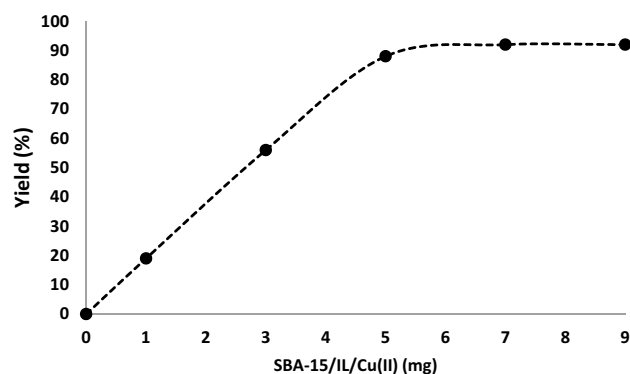


Fig. 8 Effect of increasing amount of SBA-15/IL/Cu(II) NPs on the salicyl alcohol oxidation reaction

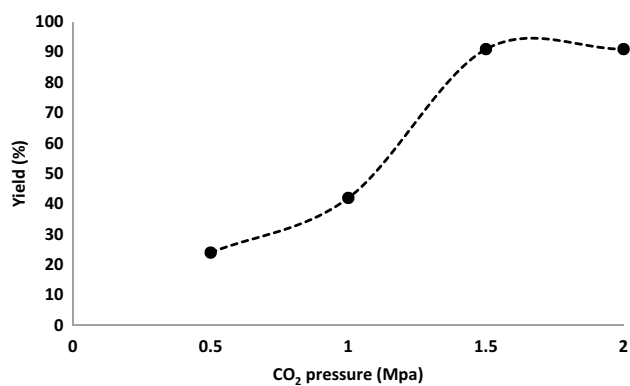


Fig. 9 Effect of CO₂ pressure on yield of salicyl alcohol oxidation reaction

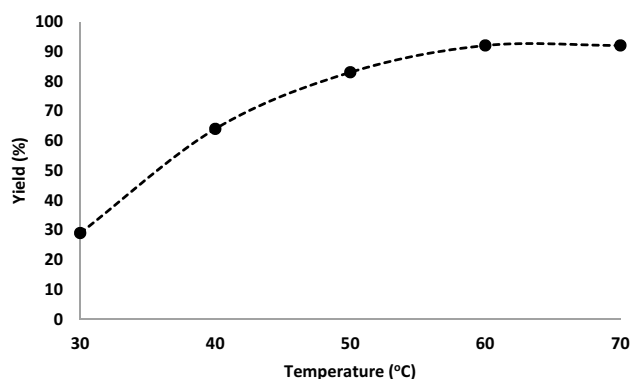


Fig. 10 Effect of temperature on yield of salicyl alcohol oxidation reaction

92% efficiency. As seen in Fig. 10, the temperature of reaction possessed a dramatic effect on the carboxylic acid yield. The carboxylic acid yield can enhance by the enhancement of reaction temperature ranging from 30 to 60 °C (92%, 60 °C) and levels off upon more enhancing temperature equal to 92 °C.

As can be seen in Table 3, in this novel one-pot approach, many aryl alcohols are studied in cases of the substrate scopes to produce carboxylic acids. Noted that, for all considered substrates, the catalyst is active. In addition, aryl alcohols bearing a para-chloro group have been introduced as proper substrates provided near-quantitative products. Aryl alcohols and also the para-bromo or para-fluoro groups, are additionally appropriate substrates. Whereas an electron-donating group like methyl over the aryl group reduced the product yield. Various aliphatic alcohols were also tested and gave the corresponding products in good yield.

For a deeper evaluation of the efficiency of the catalyst, various control experiments were conducted and the results are shown in Table 4. The reaction performed deploying SBA-15 showed that no amount of the carboxylic acid was

formed after 12 h (Table 4, row 1). Moreover, no reaction was perceived when SBA-15/IL as catalyst was employed (Table 4, row 3). IL is not able to show good catalytic activity under standard reactions. We compared the results with many other similar catalysts. Due to these unfavorable results, we continued research to increase efficiency by adding Cu (II) (Table 4, row 3). Our results show that the reaction cycle is primarily catalyzed using Cu (II) complexes in the SBA-15/IL nanostructure. Nanoparticles increase the activity of the catalyst due to the increase in surface area to volume, so they significantly increase the sensitivity between the reactants and the catalyst and act as a homogeneous catalyst (Table 4, rows 3 and 4).

On the basis of the above experiments, we proposed the mechanism in scheme 3. Firstly, the formation of carbonate ester is required to transform the hydroxyl group into a better leaving group. We find that the key features are the formation of an intermediate carbonate ester followed by nucleophilic substitution by DMSO and finally deprotonation and proton shift which leads to the aldehyde intermediate. [40] Furthermore, only CO₂ was observed after the reaction but no other reduced products of CO₂ such as HCOO–CO or HCOOH were found using neither in situ gas GC measurements. [41, 42] That supported the role of DMSO as actual oxidant. Eventually, the copper catalyst activates the intermediate to be further oxidized to carboxylic acid.

However, as determined by ICP-MS, the Cu contents in catalyst pre- and post- reaction was 1.2 and 1.1%, respectively (Table 5). This indicates that a large amount of Cu species leaching into solution are recaptured onto the fibers of SBA-15 at the end of the reaction. The main concern is the trace of other active metals (like Ni, Cd, Fe, Pd, and Co) in each component of the reaction. It was essential to perform ICP analysis of the reaction components. The concentration of Ni, Cd, Fe, Pd, and Co were very low that cast any doubt (Table 6).

In green chemistry, the catalyst reusability state is considered a significant property. Therefore, the reuse of the SBA-15/IL/Cu(II) NPs was investigated with respect to the optimal state of the synthesis of carboxylic acid. SBA-15/IL/Cu(II) solid NPs were easily isolated from the liquid reaction zone after a few seconds. The solvent can be used quickly after cleaning. As Fig. 11 illustrates, the catalyst was recycled for ten consecutive cycles. Product yield in the tenth run was 89%, showing merely a 3% decrease in performance compared to the fresh catalyst.

Furthermore, the heterogeneous essence of the catalyst was comprehensively investigated. First, a hot filtration test was performed for the synthesis of carboxylic acid under superior conditions and demonstrated that the catalyst was removed at a yield of 48% (after 6 h). After removal of the heterogeneous catalyst, it was found that the free catalyst residues were relatively active, and the

Table 3 Synthesis of carboxylic acid derivatives in the participation of SBA-15/IL/Cu(II) NPs

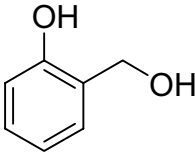
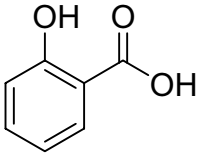
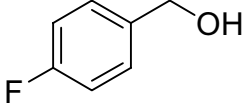
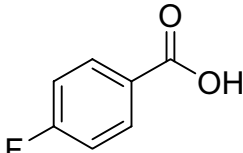
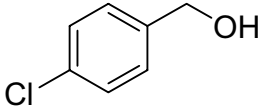
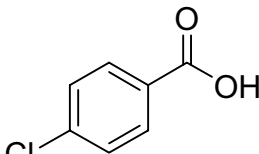
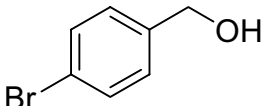
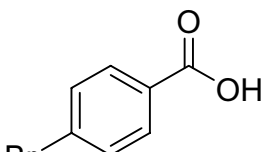
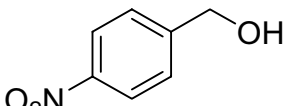
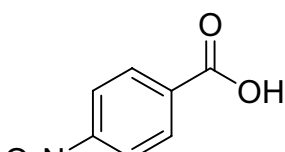
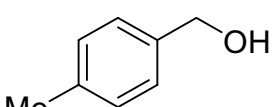
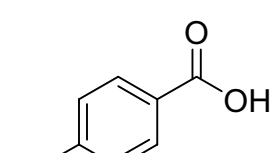
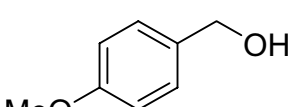
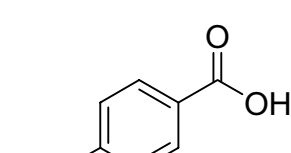
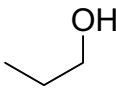
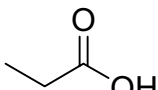
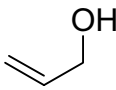
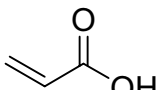
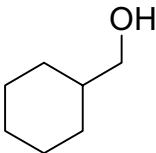
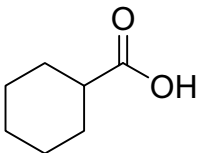
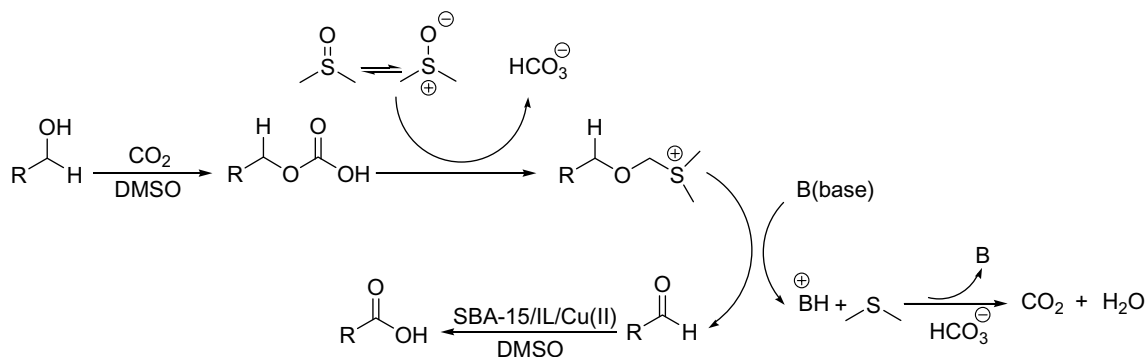
Entry	Olefins	Products	Yield (%) ^a
1			92
2			90
3			91
4			92
5			89
6			88
7			91
8			87
9			85
10			83

Table 3 (continued)Reaction conditions: alcohols (1 mmol), K_2CO_3 (5 mmol), SBA-15/IL/Cu(II) NPs (7 mg), CO_2 (1.5 MPa), DMSO (5 mL), under 60 °C^aIsolated yields**Table 4** Influence of different catalysts for synthesis of carboxylic acid

Entry	Catalyst	Yield (%) ^a
1	SBA-15	–
2	SBA-15/IL	–
3	SBA-15/IL/Cu(II)	92
4	IL/Cu(II)	91

Reaction conditions: salicyl alcohol (1 mmol), K_2CO_3 (5 mmol), SBA-15/IL/Cu(II) NPs (7 mg), CO_2 (1.5 MPa), DMSO (5 mL), under 60 °C^aIsolated yield

conversion of 51% was achieved after 12 h of synthesis of carboxylic acid. This depicted the heterogeneity of catalyst during the reaction, with partial leaching. Eventually, a Mercury-poisoning test was performed to confirm the heterogeneous nature of the catalyst. Mercury (0) significantly attenuates the metal catalyst on the active outer layer and calms its activity, confirming the heterogeneity of catalyst. This test was accomplished on the mentioned reaction model at optimal situations. After 6 h, about 300 molar mercury was released to the reaction compound and stirred. After 12 h, no alteration was perceived in the poisoned catalyst. Figure 12 depicts the kinetics of the reac-

**Scheme 3** Proposed mechanism for SBA-15/IL/Cu(II) catalyzed oxidation of alcohols**Table 5** The loading amount of Cu in SBA-15/IL/Cu(II)

Entry	Catalyst	wt %
1	SBA-15/IL/Cu(II) NPs	1.2
2	SBA-15/IL/Cu(II) NPs after ten reuses	1.1

Table 6 Chemical composition of the synthesis of carboxylic acid using ICP

Entry	Element	Weight percent (%)
1	Fe	<0.02
2	Co	–
3	Pd	<0.01
4	Cd	–
5	Ni	<0.01

tion at the attendance of Hg (0). Negative experimental outcomes illustrated that the SBA-15/IL/Cu(II) was heterogeneous and no significant copper leaching happened during synthesis of carboxylic acid.

The SEM and TEM images analyzer showed the more data in the case of the structure nanoparticles of SBA-15/IL/Cu(II). As seen in Fig. 13a and b, the TEM and SEM images for the new structure nanoparticles of SBA-15/IL/Cu(II), and the 10th structure nanoparticles SBA-15/IL/Cu(II) reused are demonstrated. The structure of tube-like related to the catalyst can be still observed after being 10th reused. The same structure between fresh nanoparticles of SBA-15/IL/Cu(II) and SBA-15/IL/Cu(II) 10th reused, observed to great power in recyclability. In addition, the thermal stability of the reused SBA-15/IL/Cu(II) catalyst after ten times recycling was not as good as that of the fresh catalyst, which might be caused by the loss of IL/Cu(II) in SBA-15 during recycling (Fig. 14). Fortunately, it did not affect its practicability when used at 100 °C.

Fig. 11 Recyclability of the catalyst

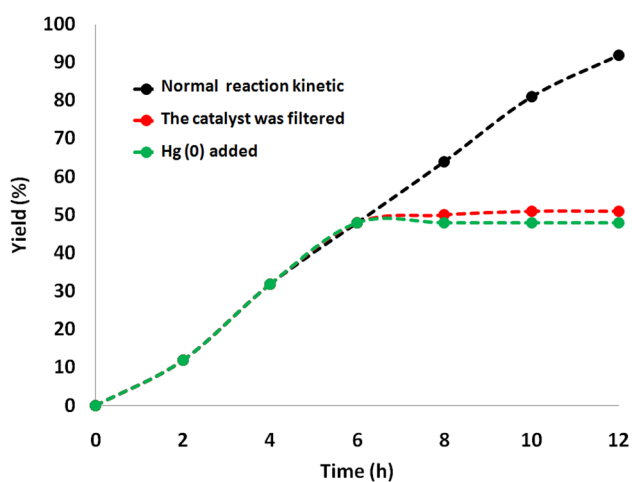
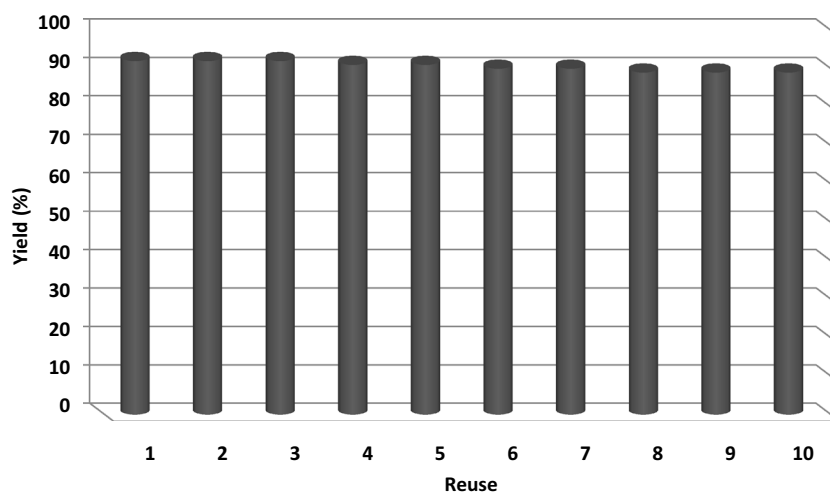
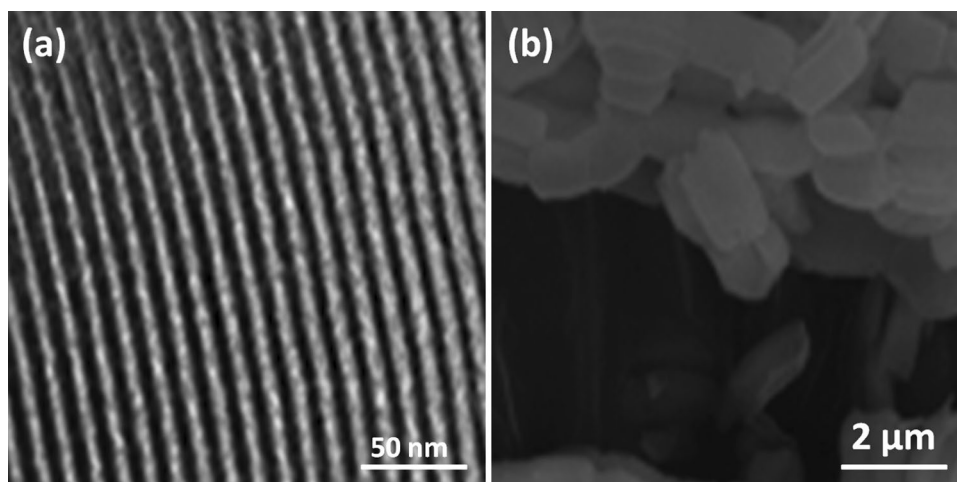


Fig. 12 Leaching test for the catalyst of synthesis of carboxylic acid

4 Conclusions

In summary, a novel class of SBA-15 mesoporous silica supported ionic liquid based on imidazole groups ligands (SBA-15/IL). Then, the recyclable SBA-15/IL supported copper (II) catalyst was synthesized that exhibited excellent catalytic activity for synthesis of carboxylic acids by the oxidation of various alcohols in excellent yields. The surface area analysis studies of BET, FTIR, TEM, XPS, SEM, TGA, ICP-MS and EDX proposed the functionalization of IL and Cu (II) in the mesopores silica surface. Moreover, the catalyst is determined to be recoverable and reusable. This rational design in the case of single-site catalysts having full utilization of each IL/Cu(II) active site and appropriate recyclability and lower catalyst leaching can occur together with the concepts of green chemistry. Hence, the investigation of SBA-15/IL/Cu(II) nanocatalyst binged an appropriate platform for fabricating other nano catalyst that is very efficient in different nano-catalyst based catalytic reactions.

Fig. 13 **a** TEM, and **b** FE-SEM images of the recovered SBA-15/IL/Cu(II) NPs after the 10 th run for synthesis of carboxylic acid



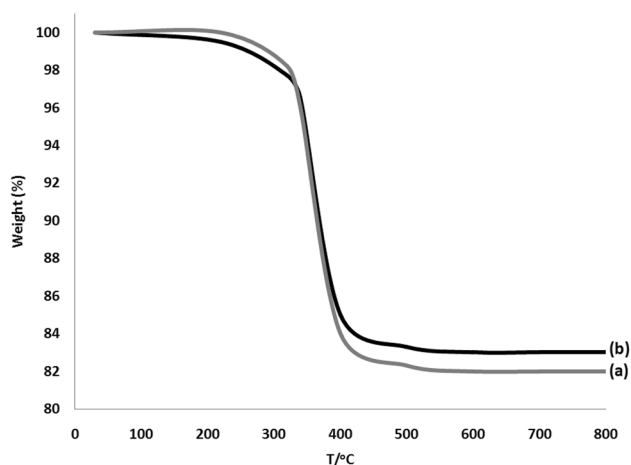


Fig. 14 TGA of the fresh SBA-15/IL/Cu(II) (a) and the reused SBA-15/IL/Cu(II) after 10 times recycling (b)

The mentioned approach can be further utilized for developing more nanocatalysts, which have appropriate properties like efficiency and simplicity of reuse.

Acknowledgements This work was financially supported by the Young Innovative Talents Project of Guangdong Provincial (No. 2020KQNCX242); the Innovative Team Program of Guangdong Province (No. 2020KCXTD057); the Guangdong Basic and Applied Basic Research Foundation (No. 2020A1515011188).

References

- Moore E, McInnes SJ, Vogt A, Voelker NH (2011) *Tetrahedron Lett* 52:2327
- Chassaing S, Sido ASS, Alix A, Kumarraja M, Pale P (2008) *Chem Eur J* 14:6713–6721
- Yousuf SK, Mukherjee D, Singh B, Maity S, Taneja SC (2010) *Green Chem* 12:1568–1572
- Lee CT, Huang S, Lipshutz BH (2009) *Adv Synth Catal* 351:3139
- Wang K, Bi X, Liao P, Fang Z, Meng X, Zhang Q, Liu Q, Ji Y (2011) *Green Chem* 13:562–565
- Chanda K, Rej S, Huang MH (2013) *Chem Eur J* 19:16036–16043
- Larin EM, Lautens M (2019) *Angew Chem Int Ed* 58:13438–13442
- Lal K, Rani P (2016) *ARKIVOC* 2016(1):307–341. <https://doi.org/10.3998/ark.5550190.p009.593>
- Kuang GC, Guha PM, Brotherton WS, Simmons JT, Stanke LA, Nguyen BT, Clark RJ, Zhu L (2011) *J Am Chem Soc* 133:13984–14001
- Harmand L, Lescure MH, Candelon N, Duttine M, Lastécouères D, Vincent JM (2012) *Tetrahedron Lett* 53:1417–1420
- Sadeghzadeh SM, Zhiani R, Moradi M (2018) *ChemistrySelect* 3:3516–3522
- Diagboya PN, Mtunzi FM, Düring RA, Olu-Owolabi BI (2021) *Ind Eng Chem Res* 60:2365–2373
- Xikhongelo RV, Mtunzi FM, Diagboya PN, Olu-Owolabi B, Düring RA (2021) *Ind Eng Chem Res* 60:3957–3968
- Sadeghi S, Karimi M, Radfar I, GhahremaniGavinehroudi R, SaberiHeydari DA (2021) *New J Chem* 45:6682–6692
- Manno R, Sebastian V, Irusta S, Mallada R, Santamaria J (2021) *Catal Today* 362:81–89
- Hu N, Ning P, He L, Guan Q, Shi Y, Miao R (2021) *Renew Energy* 170:1–11
- Hosseini HG, Doustkhah E, Kirillova MV, Rostamnia S, Mahmoudi G, Kirillov AM (2017) *Appl Catal A Gen* 548:96–102
- Rostamnia S, Doustkhah E, Zeynizadeh B (2016) *Microporous Mesoporous Mater* 222:87–93
- Rostamnia S, Golchin Hossieni H, Doustkhah E (2015) *J Organomet Chem* 791:18–23
- Rostamnia S, Doustkhah E, Bulgar R, Zeynizadeh B (2016) *Microporous Mesoporous Mater* 225:272–279
- Baghbamidi SE, Hassankhani A, Sanchooli E, Sadeghzadeh SM (2018) *Appl Organomet Chem* 32(4):e4251
- Hu YL, Zhang RL, Fang D (2019) *Environ Chem Lett* 17:501–508
- Yao N, Chen C, Li DJ, Hu YL (2020) *J Environ Chem Eng* 8:103953
- Jin T, Dong F, Liu Y, Hu YL (2019) *New J Chem* 43:2583–2590
- Sadeghzadeh SM (2015) *RSC Adv* 5:17319–17324
- Tomalia DA (2012) *New J Chem* 36:264–281
- Giocalone F, Campisciano V, Calabrese C, Parola VL, Syrgiannis Z, Prato M (2016) *ACS Nano* 10:4627–4636
- Sadjadi S, Malmir M, Heravi MM (2019) *Appl Clay Sci* 168:184–195
- Murugan E, Jebaranjitham JN, Raman KJ, Mandal A, Geethalakshmi D, Kumarc MD, Saravanakumarc A (2017) *New J Chem* 41:10860–10871
- Qin TY, Li XY, Chen JP, Zeng Y, Yu TJ, Yang GQ, Li Y (2014) *Chem Asian J* 9:3641–3649
- Hayouni S, Robert A, Maes C, Conreux A, Marin B, Mohamadou A (2018) *New J Chem* 42:18010–18020
- Balaraman E, Khaskin E, Leitus G, Milstein D (2013) *Nat Chem* 5:122–125
- Thottathil JK, Moniot JL, Mueller RH, Wong MKY, Kissick TP (1986) *J Org Chem* 51:3140–3143
- Abiko A, Roberts JC, Takemasa T, Masamune S (1986) *Tetrahedron Lett* 27:4537–4540
- Zhang L, Wu Z, Nelson NC, Sadow AD, Slowing II, Overbury SH (2015) *ACS Catal* 5:6426–6435
- Ryland BL, Stahl SS (2014) *Angew Chem Int Ed* 53:8824–8832
- Heyns K (1947) *Justus Lieb Ann Chem* 558:177
- Han L, Xing P, Jiang B (2014) *Org Lett* 16:3428–3433
- Shi Z, Su Q, Ying T, Tan X, Deng L, Dong L, Cheng W (2020) *J CO2 Util* 39:101162. <https://doi.org/10.1016/j.jcou.2020.101162>
- Wang Y, Wu ZK, Yu H, Han S, Wei Y (2020) *Green Chem* 22:3150–3154
- Riemer D, Mandaviya B, Schilling W, Götz AC, Köhl T, Finger M, Das S (2018) *ACS Catal* 8:3030–3034
- Hirapara P, Riemer D, Hazra N, Gajera J, Finger M, Das S (2017) *Green Chem* 19:5356–5360

Publisher's Note Springer Nature remains neutral with regard to jurisdictional claims in published maps and institutional affiliations.